euspen's 25th International Conference & Exhibition, Zaragoza, ES, June 2025
www.euspen.eu

Towards the development of a novel smart work-holding fixture for advanced manufacturing

Muhammad Faraz Mahmood+, Thomas Furness, Naeem Shaukat Mian, Simon Fletcher

University of Huddersfield, Queensgate, Huddersfield, HD1 3DH, UK

+*muhammadfaraz.mahmood@hud.ac.uk*

Abstract
This work highlights the initial development phase of a smart fixture that can monitor the workpiece temperature to mitigate thermal errors contributed through the work holding fixture. In machining processes, the friction generated heat by the tool-workpiece interface gets transferred to the fixture which causes thermal expansion in both the workpiece and the fixture. It has been identified that the thermal expansion of the workpiece holding fixture also contributes to further exacerbate the overall thermal accuracy of the workpiece. A Finite Element Analysis (FEA) based modelling technique was utilised for the determination of workpiece thermal deformation whilst in a work-holding system. To replicate cutting trials, controlled heat experiment was conducted where an aluminium workpiece has been considered constrained in the work holding fixture. The results from experiments were used to calculate input parameters for FEA simulations. Temperature flow directions and gradients were considered to ensure experimental gradients match simulated gradients which led to further validate both experimental and simulated thermal deformation results. The results suggested a good quantitative agreement with averaged temperature accuracy of 94.28% and thermal deformation accuracy of 89.27% in the X-axis direction and 94.98% in the Y-axis direction.

Fixture, Thermal deformation, Thermal errors, Heat, Thermally sensitive points, Simulation.

1. Introduction

Thermal errors contributes about 40-70% out of the total machining errors [1]. Additionally, 15% to 20% of the total heat generated during cutting process enters the workpiece [2] which is in direct contact to work-holding enabling heat dissipation. Therefore, it is crucial to develop advanced monitoring solutions for smart fixtures that contribute in reducing thermal errors in CNC machines. *Zhaopeng et al* [3] proposed the concept of an intelligent cutting tool integrated with thin-film thermocouple (TFTC) sensor for monitoring temperature data during CNC turning process under different working conditions. The sensor was embedded at the tool tip to monitor the temperature at the tool-chip interface during machining. *Gholamzadeh and Soleimanimehr* [4] presented a coupled FEA model (dynamic and thermal analysis) to investigate cutting force and heat generation in Ultrasonic Assisted Turning. The 28 models offered insights into the thermal and mechanical behaviours. It identified the complex interactions arising from vibratory motion of the cutting tool accounting for convection rate, heat dissipation and friction at cutting tool interface. Moreover, the FEA model had a strong agreement with experimental data showing the reliability in commercial applications. *Shulong et al* [5] proposed a novel error prediction methodology using FEA based fixture-workpiece system, cutting force modelling, and fixture based actuators to minimize geometric errors and machining deflections. However, those methods overlooked thermal errors for fixtures that are critical for further accuracy. During cutting operations, heat is generated due to friction caused at the tool-workpiece interface increasing the temperatures of the workpiece and fixture [6]. This heat dissipation causes thermal deformation leading to machining errors such as fixture instability, dimensional inaccuracies, and material property changes. Therefore, analysing the thermal effects of workpiece and fixture system is critical to minimize errors and improve machining precision. For this reason, an FEA based fixture model was developed to identify and quantify its workpiece's thermal deformation by the application of a controlled heat source based on constant end milling process.

2. Methodology and Research steps

In this research, Aluminium 6082 material was selected as a workpiece for the fixture model due to its wide engineering applications for aerospace, automobile and electronics industry respectively [7]. However, a basic slab model for steady-state thermal analysis was developed first to validate the FEA accuracy by identifying deviation in results between simulation and mathematical calculations. Steady-state thermal analysis was essential for understanding the long-term thermal behaviour of materials and components under constant operating conditions similar to constant milling. The FEA results were then compared with the heat transfer equation derived from Fourier's law of conduction Q (cond) and Newton's law of cooling Q(conv). Copper was selected in the first benchmark test to better understand the universality of the proposed software (Ansys 2023 R2®) and ensure its applicability beyond aluminium material. After obtaining the accuracy of 99.42% from the basic slab simulation, a fixture was then selected based on durability, availability, and fixture design modelling to carry out controlled heat benchmark experiment. The controlled heat experiment was the replication of end milling process consisting of continuous heat dissipation through cutting tool's friction over the workpiece's surface. The reason for applying constant heat was to create awareness of how heat can be dissipated through workpiece into the fixture during machining. The use of temperature sensors was implemented within the fixture considering the concept of integrating it with smart sensing capability for monitoring temperatures of the workpiece during the benchmark test. As the change of temperature impacts the deformation change, the thermal deformation of the workpiece was also measured through Renishaw RMP60 probe before and after the experiment. After the completion of experiment, a coupled FEA based model (transient thermal-structural analysis) of fixture was developed holding the aluminium workpiece in which a controlled heat flux was applied on workpiece's top surface similar to the experiment's heat source. Transient analysis was carried out due to the time-dependent heat transfer in controlled heat experiment that formed thermal gradients overtime. The FEA boundary conditions were then validated with acceptable accuracy for developing machining based models for studying thermal characteristics of the workpiece and fixture.

2.1. Theoretical Calculations and Simulation

This section validates the accuracy of FEA through development of a basic slab model to analyse the deviation between simulation results and theoretical calculations. The dimensions of 100 mm x 50 mm x 50 mm for copper slab were taken randomly for steady-state thermal analysis. The heat transfer simulation was carried out comparing it's results with the derived heat transfer equation. By employing Fourier's law for conduction Q(cond) (equation 2.1) and Newton's law of cooling Q(conv) (equation 2.2), equation 2.3 was obtained for comparison with the simulation results. The calculations were performed on the basis of SI (m) units' system.

$$Q(cond) = KA\frac{(T1-T2)}{\Delta x} \text{ ...... (2.1)}$$

$$Q(conv) = hA(T2 - T\infty) \text{ ...... (2.2)}$$

$$T2 = \frac{\frac{KT1}{\Delta x} + hT\infty}{\frac{K}{\Delta x} + h} \text{ ....(2.3)}$$

The simulation was set up considering the boundary conditions such as type of material, convection rate, ambient temperature, and applied thermal loads replicating the real time conditions. A constant temperature of 600°C was applied on left side plane (0.05 m length) of the copper slab similar to heat dissipation through one surface of the workpiece during milling. The reason for applying 600°C was due to its re-crystallisation phenomenon which significantly change its thermal properties [8]. The rest three side planes (0.05 m, 0.10 m, 0.10 m lengths) of the slab were left with no heat loads. By giving 22°C ambient temperature with 6 W/m2°C convection rate [9] over the whole component, thermal symmetry is generated. The same convection magnitude was followed in the controlled heat experiment. The temperature values (T1 and T2) were probed on the copper slab i.e. 600 °C and 595.6 °C respectively (figure 2.1). The FEA values were compared with hand calculations through equation 2.3 evaluating simulation's accuracy.

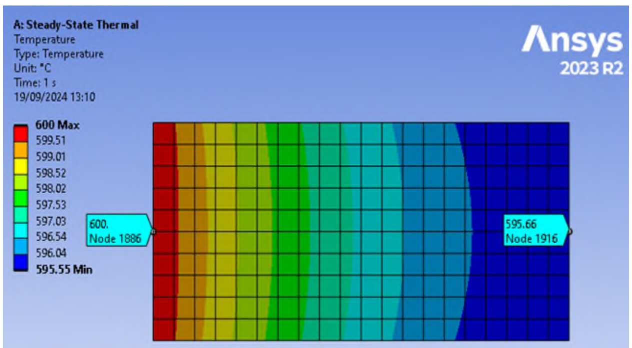

Figure 2.1. Steady-state thermal analysis

Data:

$\Delta x = 0.1$ m; $K_{(Copper)} = 400$ W/m°C

$h = 6$ W/m²°C; $T_1 = 600$°C

$T_\infty = 22$°C; $T_2 = ?$

By using the above data in equation 2.3, we get the value of T_2 as follows.

Calculation:

$$T2 = \frac{KT1/\Delta x + hT\infty}{K/\Delta x + h}$$

$$T2 = \frac{400\ x\ 600/0.1 + 6\ x\ 22}{400/0.1 + 6}$$

$$T2 = 599.13\ °C$$

As from the obtained value of T2, the benchmark calculations confirms that the result temperature of simulation is predicted with 99.42 % accuracy and also validates the use of equation 2.3. Furthermore, the comparative results ensured the reliability of using of FEA for accurate results.

2.2. Benchmark testing

This section describes the details of controlled heat test. A Positive Temperature Coefficient (PTC) heater with 55W output was utilised operated at 12-24 volts providing controlled heat source on top of the workpiece. An STC-1000 temperature controller was used to maintain the PTC at specific temperature, powered by RSPD3303X-E DC power supply. A thermistor was kept in a cavity on workpiece's top surface indicating the clamped PTC's temperature to the controller. To monitor temperature variations, five DS18B20 temperature sensors were used, providing a range of -55°C to +125°C, and ±0.5 °C accuracy [10]. A FLIR A615 thermal camera was also used to capture the thermal distribution of fixture system. The readings from the thermal camera were crucial for obtaining Body Heat Flux (BHF) for simulation, and comparison with FEA temperature results for accuracy validation. An aluminium 6082 workpiece (52.5 mm x 40.0 mm x 47.5 mm) shown in figure 2.2 was used. Masking tape was applied on fixture components to control emissivity. Emissivity value for making tape is 0.96 [11]. The majority of the workpiece portion retains temperature from 40- 60°C during cutting operation as illustrated by L Nowakowski [6]. For this reason, the PTC heater clamped to the top of workpiece and connected to the temperature controller was set to 55°C. It took 2 hours and 15 minutes (8100 seconds) reaching the target temperature. Five sensors tracked temperature changes including S1 on the workpiece side to monitor its temperature. S2 and S3 inside the machine, and S4 and S5 outside for monitoring ambient readings to implement in simulations. The thermal camera recorded temperature distribution with data used to calculate BHF of the PTC heater.

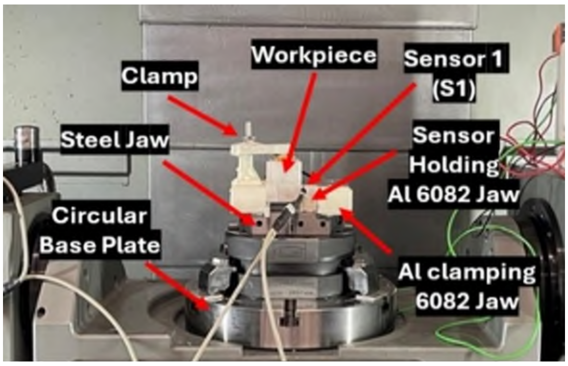

Fig 2.2. Setup details of the experiment

The thermal deformation caused due to increase in temperature was measured by probing the specified points on the workpiece with Renishaw RMP60 probe. The following figure 2.3 shows the probed locations measuring thermal deformation before and after (at 8100th second) the experiment. The probe location was set to 10 mm from workpiece centre, and 15 mm from workpiece top surface avoiding collision with the clamp whilst covering all four sides surfaces. The total deformation along X and Y axes was measured by adding deformation values from each of the two surfaces laying on the same axis.

Fig 2.3 Probing point for thermal deformation

Temperature data from the thermal camera (figure 2.4) captured readings for the PTC heater and both top and bottom of the workpiece. The DS18B20 sensors monitored temperature changes throughout the test.

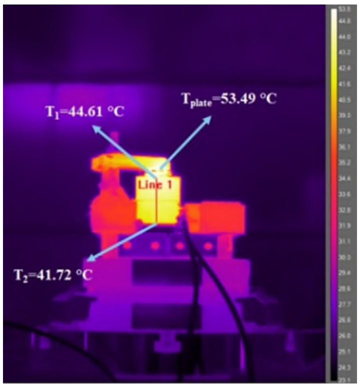

Fig 2.4. Thermal imaging

The temperatures from the DS18B20 sensors at 8100th second were measured from the experiment as shown in table 2-1.

Temperatures	Magnitudes (°C)
S1	37.0 °C
S2	22.6 °C
S3	23.3 °C
S4	23.5 °C
S5	22.8 °C
Average Ambient Temperature	23.0 °C

Tale 2-1. Temperature details of the controlled heat experiment

The temperature vs time graph of the DS18B20 sensors was plotted (figure 2.5) to monitor temperature change during the experiment.

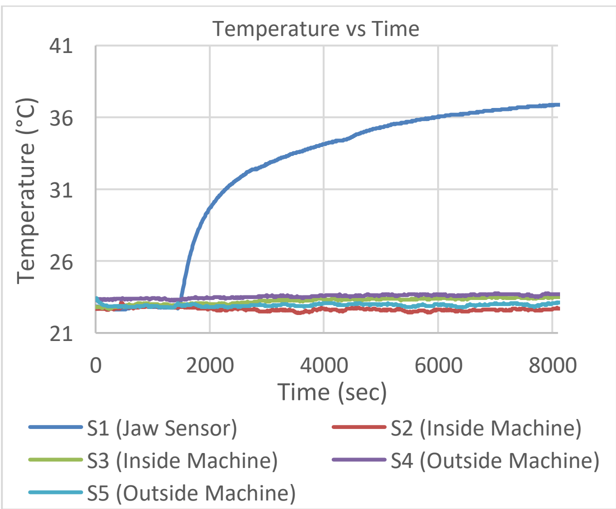

Figure 2.5. Temperature vs time graph of the temperature sensors

3. Validation

This section validates the accuracy of the controlled heat FEA simulations. The BHF value was obtained using temperature values plotted from thermal camera. The heat energy was calculated through equation 2.1 which was further divided by area of the PTC heat source to obtain BHF value. The BHF magnitude was then applied in the simulation's PTC heat source to validate the experiment.

$$Q = KA\frac{(T1-T2)}{\Delta x}$$

$$Q = (180)(0.0021)\frac{(44.6-41.7)}{0.0475}$$

$$Q = 23.077\ W$$

Now, dividing value of 'Q' by the volume of the PTC heater using equation 3.1 to obtain the BHF value;

$$Body\ Heat\ Flux = \frac{Heat\ Energy}{Volume\ of\ Heat\ Source} \ldots (3.1)$$

$$Body\ Heat\ Flux = \frac{23.077}{2.5584e-6}$$

$$Body\ Heat\ Flux = 9020090.682\,\frac{W}{m^3}$$

A CAD model of a fixture (figure 3.1) was designed including all the components similar to the 5-axis CNC machine (HURCO VMX30Ui) used in the practical experiment.

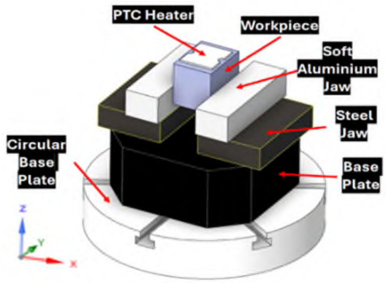

Figure 3.1. CAD Model of the controlled heat experiment

The material for steel jaws, base plate and circular base were made up of steel whose exact grades were unknown and were left as default structural steel. The BHF value was applied to the PTC in simulation. All contacts in the model were defined as bonded with asymmetric behaviour and augmented Lagrange formulation offering better computational efficiency and stability while handling contact problems. The thermal contact conductance (TCC) 1956 W/m2 °C taken from [9] applied to all contacts in the model. The simulation time was set up to 8100 seconds as per the experiment. The simulation results obtained (figure 3.2) were validated by probing temperatures at the required locations similar to real experiment thermal image. The accuracies achieved from 91.70 - 96.19% as shown in table 3-1.

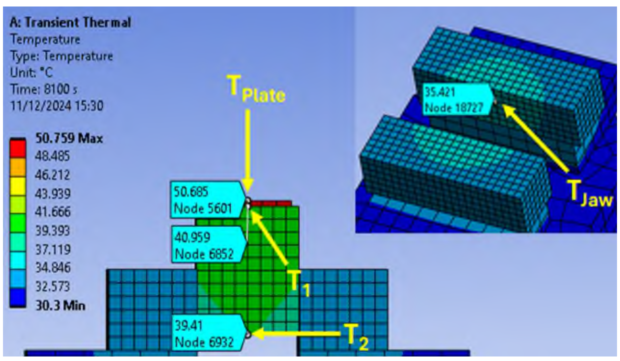

Fig 3.2. Probed Temperature points in FEA simulation

Experiment Temperatures (°C)	Simulation Temperatures (°C)	Accuracy %
T_{S1}= 36.8 °C	T_{S1}= 35.4 °C	96.19 %
T_{Plate}= 53.4 °C	T_{Plate}= 50.6 °C	94.75 %
T_1= 44.6 °C	T_1= 40.9 °C	91.70 %
T_2= 41.7 °C	T_2= 39.4 °C	94.48 %

Table 3-1. Experiment and simulation temperatures comparison

Similarly, thermal deformation was measured by probing locations in simulation similar to the experiment. The simulation results were compared with the experiment resulting with accuracy of 95.27% (X-axis deformation) and 89.48% (Y-axis deformation) as shown in table 3-2. The probed points can be shown in figure 3.3. The points were taken from all four sides of the workpiece covering total deformation from each of the two sides laying on the same axis.

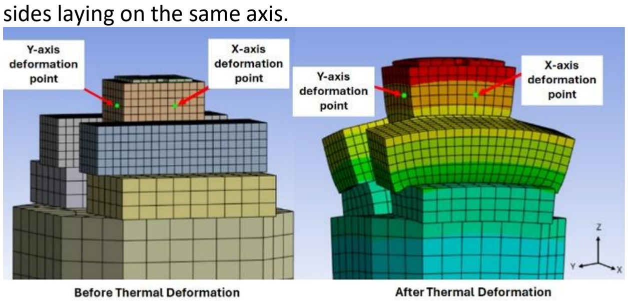

Figure 3.3. X and Y axes deformation measuring points

S. No	Probed Points	Deformation Results (µm/°C)		
		Simulation	Experiment	Accuracy %
1	x-axis deformation (expansion)	17.15	18	95.27
2	y-axis deformation (expansion)	22.37	25	89.48

Table 3-2. Experiment and simulation temperatures comparison

4. Analysis of the Uncertainty Contribution

The results obtained in this study reveals a good agreement in experimental and simulated results, however, it is important to highlight the assumptions used during FEA simulations which may have contributed to the uncertainties in results. The experimental fixture setup consisted of factors such as quality of component joints, soft jaw bolts, jaw gap size, and jaw serrations which were modelled in FEA as solid models with closely matching material properties. Similarly, modelling of air pockets, and parameters such as convection, mesh density and thermal contact conductance were assumed to be constant at a variety of places in the fixture which may not represent the true condition of the fixture. It is also noted that the accuracy of temperature sensors (±0.5°C) may also have contributed to representing the true temperature state which have affected calculations of heat flux parameters. It is believed that consideration of these uncertainties would significantly improve modelling and accuracy of results.

5. Conclusion

This research contributes towards the development of a smart work-holding fixture identifying and quantifying thermal deformations and temperatures of the workpiece. It has set the awareness of how fixtures contribute to the thermal errors in machining. An FEA modelling method was introduced for the development of fixture during milling. A controlled heat test was carried out validating the FEA modelling boundary conditions by identifying its deviation from the real experiment. The experimental results gave an effective approach to study workpiece's thermal fluctuations with its simulation results reaching an average accuracy of 94.28% for temperatures, and 89.48% and 95.27% for Y-axis and X-axis thermal deformation respectively. FEA results confirmed their reliability for machining simulations provided with optimum accuracy. This research formed the basis for developing future FEA based fixture models for machining applications provided with the concept of utilising sensors for measuring temperatures and probing for monitoring thermal deformations. It formed the foundation for enhancing practical implementation and developing fixture designs negating thermal errors for higher precision in manufacturing system. The future work should concentrate on integrating temperature and deformation sensors effectively for milling whilst developing dynamic error compensation methodologies.

6. Acknowledgement

The Authors acknowledge and thank the Advanced Machinery and Productivity Institute (AMPI) (application number 84646) who funded this work. We further thank Mr. Andrew Bell for giving all the technical help throughout the experimental work.

References

1. Bryan, J., *International status of thermal error research (1990).* CIRP annals, 1990. **39**(2): p. 645-656.
2. Moriwaki, T., *Study on Machining Error Due to Cutting Heat in Endmilling.* Mem. Grad. School Sci. & Tecnol., Kobe Univ., 1995. **13**: p. 131.
3. He, Z., et al., *Research on tool wear prediction based on temperature signals and deep learning.* Wear, 2021. **478**: p. 203902.
4. Gholamzadeh, B. and H. Soleimanimehr, *Finite element modeling of ultrasonic-assisted turning: cutting force and heat generation.* Machining Science and Technology, 2019. **23**(6): p. 869-885.
5. Liu, S., et al., *Machining error prediction scheme aided smart fixture development in machining of a Ti6Al4V slender part.* Proceedings of the Institution of Mechanical Engineers, Part B: Journal of Engineering Manufacture, 2023. **237**(10): p. 1509-1517.
6. Nowakowski, L., et al., *Influence of the cutting strategy on the temperature and surface flatness of the workpiece in face milling.* Materials, 2020. **13**(20): p. 4542.
7. Chen, J., *Research on aluminum alloy materials and application technology for automotive lightweighting.* J. Mater. Chem, 2023. **4**: p. 1-7.
8. Hossain, R. and V. Sahajwalla, *Material microsurgery: selective synthesis of materials via high-temperature chemistry for microrecycling of electronic waste.* ACS omega, 2020. **5**(28): p. 17062-17070.
9. Mian, N.S., *Efficient machine tool thermal error modelling strategy for accurate offline assessment*. 2010, University of Huddersfield.
10. Bora, D., D. Singh, and B. Negi. *Utilization of DS18B20 Temperature Sensor for Predictive Maintenance of Reciprocating Compressor*. in *2023 International Conference on Power Energy, Environment & Intelligent Control (PEEIC)*. 2023. IEEE.
11. Hagen, K.D., *Heat transfer with applications*. 1999: Prentice Hall.